Optimization of InAs/AlInAs quantum wells based up-converter for silicon solar cells

Nikola Prodanović, Jelena Radovanović, Vitomir Milanović, and Stanko Tomić

Additional information on J. Appl. Phys.

Optimization of InAs/AlInAs quantum wells based up-converter for silicon solar cells

Nikola Prodanović,[1] Jelena Radovanović,[2,a)] Vitomir Milanović,[2] and Stanko Tomić[3]

[1]*School of Electronic and Electrical Engineering, University of Leeds, Woodhouse Lane, Leeds LS2 9JT, United Kingdom*
[2]*School of Electrical Engineering, University of Belgrade, Bulevar kralja Aleksandra 73, 11120 Belgrade, Serbia*
[3]*Joule Physics Laboratory, School of Computing, Science and Engineering, University of Salford, Salford M5 4WT, United Kingdom*

We present an optimization procedure for the design of InAs/AlInAs quantum well (QW) based up-converter for silicon solar cells. By utilizing nonlinear optical effects in QW structures, the up-conversion of low energy photons for which the silicon (Si) is transparent, into higher energy photons that can be absorbed by a Si solar cell, is achieved. Due to lack of the III-V material combinations that can provide a large enough conduction band offset to accommodate three bound states required for the optimal operation, we explore the possibilities of using continuum part of the spectrum as the third state. Optimization of the up-converter is performed by maximization of the second order susceptibility derived from the density matrix formalism. Our procedure is based on use of the genetic algorithm global optimization tool, as a "driver" routine for the eight-band $\mathbf{k} \cdot \mathbf{p}$ Hamiltonian "solver" of the QW electronic structure problem. © *2011 American Institute of Physics*. [doi:10.1063/1.3641977]

I. INTRODUCTION

One of the major obstacles for high power conversion efficiency of the sun light with conventional semiconductor materials is that only photons with energies close to that of the semiconductor energy gap (E_g) are effectively converted into electron-hole pairs. Photons with energy lower than E_g are simply lost (the semiconductor is transparent to them) and of photons with higher energy ($> E_g$), only a part, i.e., those with energy almost equal to E_g are best suited for absorption. The majority of high energy electrons generated by photons with $> E_g$, (hot carriers) decay fast thermally to the conduction band Fermi level before they can contribute to the output current. The principal aim here must be to make a better use of the solar spectrum.[1–7] One of the promising concepts is to place another device, a "light converter," attached to the rear (front) of an existing solar cell (SC), to capture photons with energy below (above) the energy gap of SC and re-emit them at the higher (lower) energy to match the region where SC exhibits a very good spectral response. Thus it is possible to enhance the conversion efficiency of the SC device.[8–11] Up or down conversion can occur in a three-level quantum mechanical systems in a manner that luminescent materials convert photons by utilizing nonlinear optical effects.

In this paper, we propose utilization of the quantum well structure, optimized with respect to its nonlinear susceptibility, as a luminescent material. For a three level system, the difference between the highest and the lowest bound state has to be approximately the same as the SC (in our case Si) energy gap.

A detailed examination of the literature[12–14] proved that it was almost impossible to find well/barrier material combination among conventional III-V binaries and their alloys; which can provide for deep enough conduction band offset to accommodate at least three bound states, sufficiently spaced for 1.12 eV (Si energy gap) conversion. The main obstacle here was the appearance of indirect bands (originating from X or L states) in the barrier materials beyond certain Al concentration in Al containing ternaries. Therefore, the continual part of the spectrum has to be used instead as the third state. We have chosen $Al_{0.6}In_{0.4}As$ as a barrier and InAs as a well material for the design of the optical up-converter. Optimization of the QW based up-converter is performed by using the genetic algorithm (GA) as a global optimization tool,[15–18] to maximize the second order nonlinear susceptibility by varying the QW structural parameters. The quantum well electronic states, wavefunctions, and optical dipole matrix elements needed to determine the nonlinear susceptibility were calculated from the eight-band $\mathbf{k} \cdot \mathbf{p}$ model that takes into account conduction to valence band band mixing as well as the effect of strain.

II. THEORETICAL CONSIDERATIONS

A. Genetic algorithm

Owing to the complexity of the target function of an up-converter, it would be very difficult to find its global maximum within given multidimensional domain by using classical optimization algorithms like downhill simplex or conjugate gradients[19] or specialized methods[20] including isospectral transformations of the Hamiltonian.[21–23] Therefore we formulate our method using the global optimization tool based on the genetic algorithm (GA).[24] Genetic algorithm is

---

a global optimization search engine for the maximization of scalar functions, $f(x_1, x_1, \ldots, x_n)$, of real vector arguments, $(x_1, \ldots, x_n)$, where n is the number of independent parameters. The optimization mechanism behind the genetic algorithm can be understood analogously to the evolution of a biological system, i.e., a population of individuals. In such a system, evolution is interpreted as an optimization of certain fitness properties of the population.

In GA, the population is represented by a set of points $(x_1^i, x_1^i, \ldots, x_n^i)$, in the parameter space, where $i = 1 \ldots n_p$ and n_p is the population size. The algorithm starts from an initial population that is randomly chosen. The average value of the fitness (target) function in the initial population (for the initial set of parameters) can be very small, but it is expected to reach an optimal value through the evolutionary process (optimization). Starting from this initial population, the algorithm produces a new generation ("siblings") in every subsequent iteration through the process of reproduction. Reproduction entails selection of two parents from a previous generation, and this is done stochastically, with probability proportional to the fitness, i.e., target value of the individuals in the old generation. The number of iterations in the GA can be fixed and should be set to a high enough value so that the algorithm may reach a predefined convergence criteria before termination.

B. Electronic structure model

To calculate the electronic structure of the up-converter, we have used the 8-band $\mathbf{k} \cdot \mathbf{p}$ Hamiltonian,[25] which at $k_\parallel = 0$ can be reduced to:

$$H = \begin{pmatrix} G & 0 \\ 0 & G \end{pmatrix} \quad (1)$$

with

$$G = \begin{pmatrix} E_{cb}(z) & 0 & \sqrt{2}\hat{U} & -\hat{U} \\ 0 & E_{hh}(z) & 0 & 0 \\ \sqrt{2}\hat{U}^\dagger & 0 & E_{lh}(z) & Q(z) \\ -\hat{U}^\dagger & 0 & Q^\dagger(z) & E_{so}(z) \end{pmatrix}$$

and

$$\hat{U} = \frac{\hbar}{\sqrt{6m_0}}\sqrt{E_P}\frac{d}{dz} \quad (2)$$

$$Q(z) = -\sqrt{2}\zeta(z) \quad (3)$$

$$E_{cb}(z) = E_{c0} + 2a_c(z)\left[1 - \frac{c_{12}(z)}{c_{11}(z)}\right]\varepsilon_{xx}(z) \quad (4)$$

$$E_{lh/hh}(z) = E_{v0} + 2a_v(z)\left[1 - \frac{c_{12}(z)}{c_{11}(z)}\right]\varepsilon_{xx}(z) \pm \zeta(z) \quad (5)$$

$$E_{so}(z) = E_{v0} - \Delta_{so}(z), \quad (6)$$

where $\zeta(z) = -b_{ax}(z)[1 - c_{12}(z)/c_{11}(z)]\varepsilon_{xx}$ is the shear strain, E_{c0} and E_{v0} represent the bottom of the conduction band and the top of the valence band of the unstrained bulk material, respectively, and m_0 is the free electron mass. Furthermore, E_P is the Kane energy, which is assumed to be z-independent and to take an average value throughout the structure, Δ_{so} is the spin-orbit splitting energy, b_{ax} is the axial deformation potential, and a_c and a_v are the hydrostatic deformation potentials for conduction and valence band, respectively. Finally, c_{11} and c_{12} stand for the elastic constants of the crystals that constitute the structure, while $\varepsilon_{xx} = (a_b - a_w)/a_w$ is the relative change in the lattice constants at the barrier-well interface, with a_b and a_w being the lattice constants of the bulk barrier and well material. The solution of the Hamiltonian eigenvalue problem:

$$\begin{pmatrix} E_{cb} & 0 & \sqrt{2}U & -U \\ 0 & E_{hh} & 0 & 0 \\ \sqrt{2}U^\dagger & 0 & E_{lh} & Q \\ -U^\dagger & 0 & Q^\dagger & E_{so} \end{pmatrix}\begin{pmatrix} \phi_c \\ \phi_{hh} \\ \phi_{lh} \\ \phi_{so} \end{pmatrix} = E\begin{pmatrix} \phi_c \\ \phi_{hh} \\ \phi_{lh} \\ \phi_{so} \end{pmatrix}, \quad (7)$$

can be found in an analytic form for a layered structure. From Eq. (7), we obtain a Schrödinger like equation for $\phi_c(z)$

$$-\frac{\hbar^2}{2}\frac{d}{dz}\frac{1}{m^*(E,z)}\frac{d}{dz}\phi_c(z) + E_{cb}(z)\phi_c(z) = E\phi_c(z), \quad (8)$$

with

$$m^*(E,z) = 3m_0^*(z)m_0$$
$$\times \frac{[E - E_{lh}(z)][E - E_{so}(z)] - 2\zeta^2(z)}{E_g(z)\{2[E - E_{so}(z) + 2\zeta(z)] + [E - E_{lh}(z)]\}} \quad (9)$$

where $E_g(z) = E_{c0}(z) - E_{v0}(z)$, while $m_0^*(z) = E_g(z)/E_p$ is the parabolic effective mass given in Table I. If $\zeta = 0$, $a_b = a_w$ and $E_{so} = E_{lh}$, then Eq. (9) reduces to the well-known expression for nonparabolic effective mass (Ref. 26): $m^*(E,z) = m_0^*(z)m_0\left[1 + (E - E_{c0}(z))/E_g(z)\right]$.

TABLE I. The properties of AlAs and InAs used in calculations of layer parameters and electronic structure of the convertor (Refs. 12 and 13). VBO is the top of the valence band within the scale where VBO of InSb is set to zero.

	AlAs	InAs
a_0 [nm]	0.56611	0.60583
m_0^* [m_0]	0.15	0.026
E_g [eV]	3.01	0.359
E_p [eV]	21.1	21.5
VBO [eV]	−1.33	−0.59
Δ_{so} [eV]	0.28	0.39
a_c [eV]	−5.64	−5.08
a_v [eV]	−2.47	−1
b_{ax} [eV]	−2.3	−1.8
c_{11} [GPa]	1250	832.9
c_{12} [GPa]	534.1	452.6

The other envelope function components can be obtained from the solution of Eq. (8) as:

$$\phi_{lh}(z) = \frac{\sqrt{2}[E_{so}(z) - E] - \sqrt{2}\zeta(z)}{[E_{lh}(z) - E][E_{so}(z) - E] - 2\zeta^2(z)}\hat{U}\phi_c(z) \quad (10)$$

$$\phi_{so}(z) = -\frac{[E_{lh}(z) - E] - 2\zeta(z)}{[E_{lh}(z) - E][E_{so}(z) - E] - 2\zeta^2(z)}\hat{U}\phi_c(z), \quad (11)$$

and $\phi_{hh}(z)$ is decoupled at $k_{\parallel} = 0$.

It has been shown in Ref. 27 that the normalization condition for the ith state is given as:

$$1 = \langle\phi_{c,i}|\phi_{c,i}\rangle + \langle\phi_{so,i}|\phi_{so,i}\rangle + \langle\phi_{lh,i}|\phi_{lh,i}\rangle \quad (12)$$

and the dipole matrix elements read

$$\langle\psi_i|Z|\psi_j\rangle = \langle\phi_{c,i}|z|\phi_{c,j}\rangle + \langle\phi_{so,i}|z|\phi_{so,j}\rangle + \langle\phi_{lh,i}|z|\phi_{lh,j}\rangle \quad (13)$$

where ψ_i and ψ_j are ith and jth eigenstate of the 8-band Hamiltonian with components $\phi_{c,i}$, $\phi_{so,i}$, $\phi_{lh,i}$ and $\phi_{c,j}$, $\phi_{so,j}$, $\phi_{lh,j}$, respectively, and Z is the z coordinate operator represented as $Z = z||I||$ (I is the 3×3 unity operator).

All the equations in this section are derived for $k_{\parallel} = 0$, hence Eq. (9) is used to describe the effective mass $m^*(E, z)$, which includes the nonparabolic correction in addition to the conduction band-edge mass $m_0^*(z)m_0$. Among the quantities needed for evaluating the nonlinear optical susceptibility $\chi_{zzz}^{(2)}$, which is the main goal of this work, are the diagonal matrix elements ρ_{ll}^0 of the density matrix of the unperturbed system as described in the next section. These matrix elements may be found from 8×8 Hamiltonian for all $k_{\parallel} \neq 0$ via an extremely complex procedure. Therefore we have used two standard approximations: first, that the dependence of dipole matrix elements on $k_{\parallel}$ is very weak, so that we may consequently use their $k_{\parallel} = 0$ values, and second, that $\rho_{ll}^0 = 1$ for $l = 1$, otherwise $\rho_{ll}^0 = 0$. In this case, it is sufficient to analyze the 8×8 Hamiltonian for $k_{\parallel} = 0$ only.

C. The target function model

If we expose an electronic system such as the optical converter to the incident radiation with electric field $\mathbf{E}(\mathbf{r}, t)$, then the response can be quantified via global polarization $\mathbf{P}(\mathbf{r}, t)$ of the system. Consequently, we define the linear susceptibility χ (the first term in the response expansion) and the tensor of nonlinear susceptibility χ_{ijk} (the second term in the response expansion) through the relation:

$$P_i = \chi E_i + \sum_{j,k}\chi_{ijk}E_jE_k. \quad (14)$$

Our aim here is to derive an expression for the polarization of electronic system, which depends on quadratic terms of the electric field, starting from the calculated electronic structure of the optical converter. Then it would be possible to obtain the second order susceptibility from such expression as a target function that will be used in the optimization process.

We use the density matrix formalism to describe the electronic system of the optical converter.[28] The electric field of the incident radiation is treated as a perturbation that excites the electrons to higher states of our QW structure. New collective electron state is described by the density matrix whose matrix elements are calculated using the perturbation theory. The susceptibility tensor then reads (Ref. 28):

$$\chi_{ijk}^{(2)}(E_p, E_q, E_p + E_q) = -\frac{e^3\tilde{\rho}}{2}\sum_{lmn}\rho_{ll}^0$$

$$\times \left\{\frac{r_{ln}^i r_{nm}^j r_{ml}^k}{[(E_{nl} - E_p - E_q) - i\Gamma_{nl}][(E_{ml} - E_p) - i\Gamma_{ml}]}\right.$$

$$+ \frac{r_{ln}^i r_{nm}^k r_{ml}^j}{[(E_{nl} - E_p - E_q) - i\Gamma_{nl}][(E_{ml} - E_q) - i\Gamma_{ml}]}$$

$$+ \frac{r_{ln}^k r_{nm}^i r_{ml}^j}{[(E_{mn} - E_p - E_q) - i\Gamma_{mn}][(E_{nl} + E_p) + i\Gamma_{nl}]}$$

$$+ \frac{r_{ln}^j r_{nm}^i r_{ml}^k}{[(E_{mn} - E_p - E_q) - i\Gamma_{mn}][(E_{nl} + E_q) + i\Gamma_{nl}]}$$

$$+ \frac{r_{ln}^j r_{nm}^i r_{ml}^k}{[(E_{nm} + E_p + E_q) + i\Gamma_{nm}][(E_{ml} - E_p) - i\Gamma_{ml}]}$$

$$+ \frac{r_{ln}^k r_{nm}^i r_{ml}^j}{[(E_{nm} + E_p + E_q) + i\Gamma_{nm}][(E_{ml} - E_q) - i\Gamma_{ml}]}$$

$$+ \frac{r_{ln}^k r_{nm}^j r_{ml}^i}{[(E_{ml} + E_p + E_q) + i\Gamma_{ml}][(E_{nl} + E_p) + i\Gamma_{nl}]}$$

$$+ \left.\frac{r_{ln}^j r_{nm}^k r_{ml}^i}{[(E_{ml} + E_p + E_q) + i\Gamma_{ml}][(E_{nl} + E_q) + i\Gamma_{nl}]}\right\} \quad (15)$$

where cartesian indexes i, j, k are to be permuted as described in Ref. 28 (it should also be noted that the z component of the dipole matrix element is significantly larger than x and y components[29]), $\tilde{\rho}$ is the mean value of the electron density in the structure, ρ_{ll}^0 is the diagonal matrix element of the density matrix of the unperturbed system, r_{ln}^i is the ith component of the matrix element between states l and n, E_{nl} is the energy difference between states n and l, $E_{nl} = E_n - E_l$, Γ_{nl} is the relaxation factor between states n and l, while E_p and E_q are the relevant photon energies of radiation involved in the nonlinear effect.

Let us consider the QW up-converter with two bound states: E_1 and E_2. The energy of the first of two incident photons, E_p, that take part in the nonlinear effect, has to match the energy difference between these two bound states to excite electrons from the first to the second bound state, $E_p = E_2 - E_1$. Furthermore, as a third state involved in the nonlinear process in Eq. (15), we have to choose a state in the continuum, E_r, because we could not find any suitable material combination among III–V binaries to support all bound states. This continuum state is taken as a minimal energy that still satisfies the transparency condition $T(E) = 1$. The relaxation of an electron from E_r to the ground state, E_1, needs to produce a photon with the energy that matches the energy of the silicon SC bandgap, i.e.,

$E_r = E_g^{Si} + E_1$. At the same time, the second incident photon, E_q, needs to excite the electron from the second bound state to E_r, i.e., $E_q = E_r - E_2$. We assume that almost all electrons in the conduction band of the converter are in the ground bound state prior to exposing the convertor to the incident radiation. It is reasonable to expect that such population can be obtained by adequate doping of the structure, while still having enough electrons for optical effects to be observable. Hence, $\rho_{ll}^0 = 1$ for $l = 1$ and $\rho_{ll}^0 = 0$ for $l \neq 1$ so that the summation in Eq. (15) over l vanishes and $l = 1$. The coordinate matrix element for transitions between continuous states may be neglected; this implies that the summation over m in Eq. (15) vanishes as well and $m = 2$. The relaxation parameters Γ_{nm} between states n and m are taken to be the same for all bound to continuum state transitions and are labeled with Γ_{c1}, while parameters for bound to bound state transitions are labeled with Γ_{21}. It can also be shown that the dominant term of Eq. (15) is:

$$\chi_{zzz}^{(2)}(E_p, E_q, E_p + E_q) = -\frac{e^3 \tilde{\rho}}{2} \sum_{n>2} z_{1n} z_{n2} z_{21}$$

$$\times \left\{ \left[\frac{1}{(E_{n1} - E_p - E_q) - i\Gamma_{c1}} + \frac{1}{(E_{n2} + E_p + E_q) + i\Gamma_{c1}} \right] \right.$$

$$\times \left[\frac{1}{(E_{21} - E_p) - i\Gamma_{21}} + \frac{1}{(E_{21} - E_q) - i\Gamma_{21}} \right]$$

$$+ \left[\frac{1}{(E_{2n} - E_p - E_q) - i\Gamma_{2n}} + \frac{1}{(E_{21} + E_p + E_q) + i\Gamma_{21}} \right]$$

$$\left. \times \left[\frac{1}{(E_{n1} + E_p) + i\Gamma_{c1}} + \frac{1}{(E_{n1} + E_q) + i\Gamma_{c1}} \right] \right\} \quad (16)$$

where $z_{nm} = r_{nm}^z$, is the z component of the dipole matrix element. Because $E_{2n} < 0$, $E_{21} > 0$, and $E_{n1} > 0$, the second term in Eq. (16) can be neglected because it is far from the resonance. Also, the term $[(E_{n2} + E_p + E_q) + i\Gamma_{c1}]^{-1}$ is much smaller then $[(E_{n1} - E_p - E_q) - i\Gamma_{c1}]^{-1}$ and can be neglected too. The polarization and the electric field vectors are real quantities that imply that nonlinear susceptibility also has to be a real quantity. Therefore only the real part of Eq. (16) has to be evaluated. By taking all the previous considerations into account we obtain:

$$\chi_{zzz}^{(2)}(E_p, E_q, E_p + E_q) = \frac{e^3 \tilde{\rho} z_{21}}{2} \sum_{n>2} z_{1n} z_{n2}$$

$$\times \left\{ \frac{\Gamma_{c1}[(E_p - E_q)^2 + 2\Gamma_{21}^2] - \Gamma_{21}(E_p - E_q)(E_{n1} - E_p - E_q)}{\Gamma_{21}[(E_{n1} - E_p - E_q)^2 + \Gamma_{c1}^2][(E_p - E_q)^2 + \Gamma_{21}^2]} \right\} \quad (17)$$

Because our up-converter design is limited by having only two bound states, the remaining sum over the continuum states index n can be transformed into integration: $\sum_n \rightarrow (L_z/2\pi) \int dk_z$, where L_z is the length of the structure. By using the relation $E(k_\parallel = 0) = \hbar^2 k_{z_b}^2/2m_b^*(E) + U_b$, the integration in k space can be transformed into integration over energies of the degenerate continuum states. Here, subscript b denotes the barrier layer and U_b is the conduction

band offset between the barrier and the well material. The final expression for the second order susceptibility, to be used as the target function in GA, reads:

$$\chi_{zzz}^{(2)}(E_p, E_q, E_p + E_q) = \left| \frac{e^3 \tilde{\rho}}{\sqrt{2}\pi\hbar} z_{21} \int_{U_b}^{\infty} D(E) dE \right| \quad (18)$$

where

$$D(E) = \frac{\left[\frac{1}{2}\left(\frac{\Delta E}{\Gamma_{21}}\right)^2 + 1 \right] - \frac{1}{2}\left(\frac{\Delta E}{\Gamma_{21}}\right) \frac{E - E_r}{\Gamma_{c1}}}{\Gamma_{21} \left[\left(\frac{\Delta E}{\Gamma_{21}}\right)^2 + 1 \right]}$$

$$\times \Lambda(E)\Theta(E) \frac{(E - U_b)\frac{dm_b^*(E)}{dE} + m_b^*(E)}{\sqrt{m_b^*(E)(E - U_b)}} \quad (19)$$

and

$$\Lambda(E) = \tilde{z}_{1E_a}\tilde{z}_{2E_a} + \tilde{z}_{1E_b}\tilde{z}_{2E_b} \quad (20)$$

$$\Theta(E) = \frac{\Gamma_{c1}}{(E - E_r)^2 + \Gamma_{c1}^2}, \quad (21)$$

$$\Delta E = E_p - E_q \quad (22)$$

Here, E_a, E_b are the two orthogonal continuum double degenerate states with energy E. To prevent singularities in the limit $L_z \rightarrow \infty$, we introduce notation $\tilde{z}_{2E_{a,b}} = z_{2E_{a,b}}\sqrt{L_z}$ that allows for the factor L_z, arising from the density of continuum states, to be canceled out with the squared normalization factor of the continuum states L_z^{-1} originating from the expression for $\Lambda(E)$. One must also indicate that the function $\Lambda(E)$ does not depend on the selection of the basis states in the double degenerate subspace of the eigenvalue E with indices a and b.

We must also point out that many body effect have been neglected in our model, so $\chi_{zzz}^{(2)}$ has a linear dependence on the carrier density $\tilde{\rho}$. This approximation is valid for very low carrier densities (implicitly assumed here). For that reason, the numerical results are presented for the quantity $\chi_{zzz}^{(2)}/\tilde{\rho}$, seemingly independent of $\tilde{\rho}$. For higher values of $\tilde{\rho}$, the problem should be analyzed by using many body theory, as described in detail in Refs. 30–33. Certainly, the calculated results would quantitatively differ in that case in accordance with the increase of carrier densities. The exact determination of $\chi_{zzz}^{(2)}$ in the presence of many body effects will be presented elsewhere.

III. RESULTS AND DISCUSSION

A. Optimization of the QW based up-convertor structures

To find the optimal QW up-converter design, we have examined two types of QW structures. The first type is a layered structure where the Al content is varied independently in all the layers except the first one (which forms the deepest part of QW and is made of pure InAs). In each subsequent optimization, the number of layers was increased to 2, 3,…,

and overall improvement in the target susceptibility function was monitored. Those wells will further be referred to as the "one-step QW" for two layers, "two-steps QW" for three layers, and so on. The second type of QW structures is also layered but made of two materials only, $Al_{0.6}In_{0.4}As$ as the barrier and InAs as the well material. These structures will be labeled as a "double QW," "triple QW," etc.

For every compound layer, the material parameters to be used in Eq. (7) are obtained by linear interpolation of relevant AlAs and InAs data listed in Table I.[12,13] The relaxation parameter between the bound states is assumed to be $\Gamma_{12} = 0.005$ eV, and all the relaxation parameters between continuum and bound states are taken as $\Gamma_{c1} = 0.02$ eV. In general, the values of relaxation parameters $\Gamma_{m,n}$ depend on the structural profile, carrier density, and temperature, as specified in Ref. 34 and may vary significantly (see Fig. 6 therein). The same is to be expected for the structure analyzed in this work. However, for transitions between two bound states (1 and 2), we have settled on the typical estimate of 5 meV used in the literature. For bound-continuum transitions, the linewidths $\Gamma_{c1}(k_z)$ and $\Gamma_{c2}(k_z)$ are assumed equal and amount to 20 meV, which is significantly larger than Γ_{12}, to account for the dominant effect of transmission peak width $T(k_z)$ on line broadening. The exact approach given in Ref. 34 would undoubtedly yield different and more precise values of parameters $\Gamma_{m,n}$, dependent on the wave-vector component k_z, nonetheless, the theory presented in this work could straightforwardly be adapted for such case.

Optimization of all the structures was performed by the genetic algorithm. In case of multi-steps QW structures, we vary the content of Al and the layer width in each of the step regions. It gives, in total, three free parameters for the one-step QW, five parameters for the two-step QW, and in general, $n_p = 2n_s + 1$ parameters, where n_s is the number of steps in the well. The Al mole fraction, x, in the step regions is limited to $x \in [0, 0.6]$. This still provides structures with acceptably low strain and direct energy bandgap in the barrier region. The lower boundary for the layer width is set to one monolayer (~ 0.3 nm) while the highest value is limited by the critical layer thickness caused by the strain.[35]

In case of double QW structures, we vary only the layer widths of $Al_{0.6}In_{0.4}As$ and InAs, while the boundaries for the optimization parameters are chosen in the same manner as for the step QW structures. In this case, the total number of optimization parameters is $n_p = n_l$, where n_l is the number of layers in the structure. Optimization was also performed for the triple QW and QWs with higher number of layers.

In Fig. 1, the evolution of the susceptibility target function for the step QW is presented. The population (number of individual quantum wells being tested in each cycle for optimal value of $\chi_{zzz}^{(2)}$) is fixed to a typical value of 100, verified as suitable for problems of this type.[18,36] For each generation, the value shown is selected as the highest among 100 members of the population in the optimization process. Maximum generations rule was used as the termination criterion, implying that GA stops when a specified number of generations have evolved (in our case 500 generations is sufficient). As the population evolves, its individuals become more and more similar, as evident from Fig. 1, and the optimization
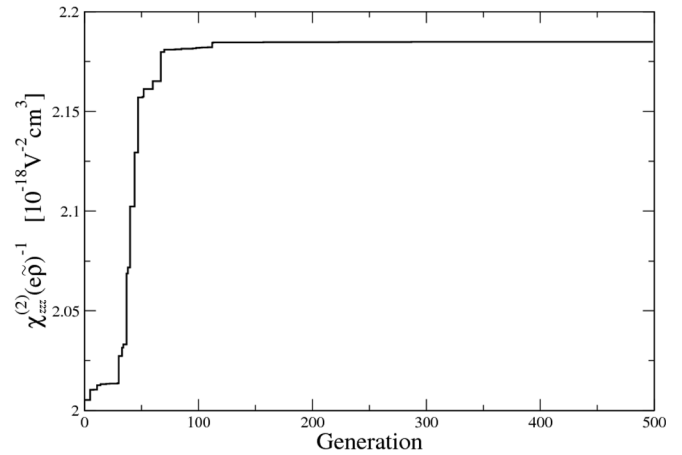

FIG. 1. The evolution of the scaled target function toward the optimal value. The vertical axis provides the maximum value of the susceptibility $\chi_{zzz}^{(2)}$ per mean density of the electron charge in the structure ($e\tilde{\rho}$) in each cycle of the genetic algorithm. Each optimal value point referrs to the best individual among the current population, and the quantity $e\tilde{\rho}$ is subject to doping. The horizontal axis indicates the number of cycles (generations). The population size is set to 100 individuals, i.e., 100 QWs in each generation, covering the free parameters space. The maximum number of generations is used as a termination criterion and 500 generations prove sufficient for a successful optimization procedure.

process ends after completing 500 cycles, having selected an optimal individual.

The resulting one-step QW, that correspond to the maximal susceptibility $\chi_{zzz}^{(2)}/e\tilde{\rho} = 2.185 \times 10^{-18} cm^3 V^{-2}$, is shown in Fig. 2. The layer widths are 2.23 nm and 3.5 nm, and the Al concentration in the step is 0.55. The energies amount to $E_1 = 0.39$ eV, $E_2 = 0.95$ eV, and $E_r = 1.51$ eV. It should be noted that in this structure, the widths of all the layers taken with arbitrary accuracy during the optimization. However, if we apply the technological constraint that the width of each layer must be an integer multiple of one monolayer, the target function reduces to $\chi_{zzz}^{(2)}/e\tilde{\rho} = 0.892 \times 10^{-18} cm^3 V^{-2}$, which is 2.45 times smaller than in the previous case. This is still a satisfactory result, and with such modification, the layer widths become equal to 2.121 nm (7 monolayers) and 3.504 nm (12 monolayers), and Al concentration is 0.55. The energy spectra are: $E_1 = 0.41$ eV $E_2 = 0.96$ eV $E_r = 1.53$ eV.
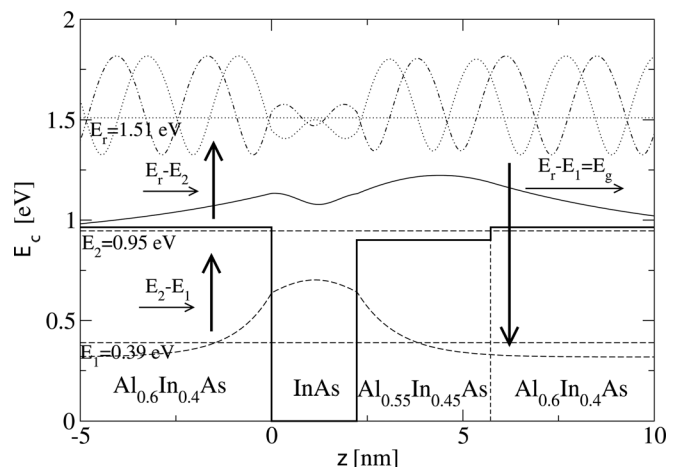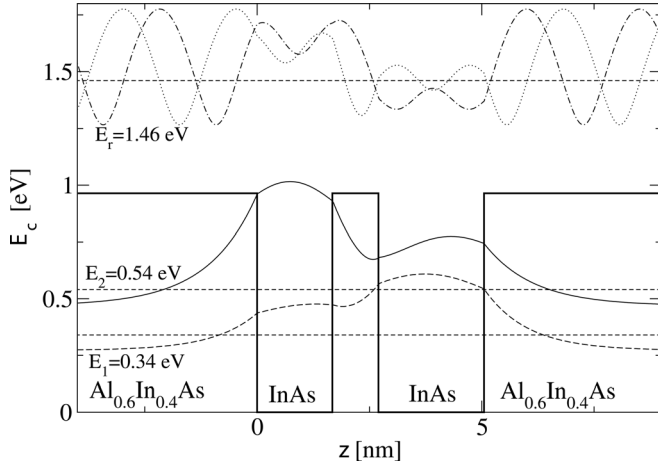

FIG. 2. The optimized step QW with respect to $\chi_{zzz}^{(2)}$.

FIG. 3. The optimized double QW with respect to $\chi^{(2)}_{zzz}$.

An alternative way to model the up-converter is by optimizing multi-QW structures with only two different kinds of materials. In such structures, we can vary only the widths of the layers and the number of layers is always odd starting from 3. Optimization procedure based on GA leads to an optimal double well structure with $\chi^{(2)}_{zzz}/e\tilde{\rho} = 0.993$ $\times 10^{-18}\text{cm}^3\text{V}^{-2}$, which is presented in Fig. 3. The layer widths are 1.689/**1.022**/2.341 nm, the Al concentration is 0.6, while the energies are at $E_2 = 0.34$ eV $E_1 = 0.54$ eV, and $E_r = 1.46$ eV. The maximal susceptibility $\chi^{(2)}_{zzz}$ of the optimized double well structure is 2.2 times lower than that of the step well. Again, after imposing technological constraints and rounding up the width of the layers to the integer multiple of one monolayer, the value of the target function reduces 1.15 times to $\chi^{(2)}_{zzz}/e\tilde{\rho} = 0.864 \times 10^{-18}$ cm^3V^{-2}. The layer widths are now: 1.515/**1.164**/2.121 nm, i.e., 5, 4, and 7 monolayers, respectively, with Al concentration of 0.6, and $E_1 = 0.38$ eV, $E_2 = 0.57$ eV, $E_r = 1.5$ eV. In comparison to the step quantum well, the $\chi^{(2)}_{zzz}$ of the optimized double well with layers widths limited to the integer number of one monolayer has 2.55 times lower value. This is again an acceptable result, bearing in mind that in an arbitrarily chosen QW $\chi^{(2)}$ can be several orders of magnitude lower.

To check out if the structures with larger number of layers or steps can provide for the increased susceptibility, we have performed further optimizations of two-step, three-step as well as triple QW structures. We have observed that those more complex structures improve the susceptibility for only $\sim$5% when compared to the one-step or double QW structures. Hence, it is probably not worth the technological effort to grow structures with increased number of layers due to negligible improvement of the desired effect. Thus for the multi-step wells structures, the optimal solution appears to be a one-step well. Furthermore, for the second type of structures, the optimal one is the simple double well with three layers.

We conclude that the optimized QW structure presented in Fig. 2 has the highest value of the target susceptibility function among all the layered structures considered here.

To obtain the overall efficiency improvement, it is necessary that the absolute value of the photon flux emitted from the SC to the converter does not exceed the photon flux emitted from the converter and absorbed by SC. This implies that the SC chemical potential μ_{sc} should be smaller then the chemical potential of emitted light from the up-converter μ_c. Because the chemical potential of the radiation cannot exceed the lowest photon energy that forms the radiation, we have: $\mu_c < U_b - E_2$.[8] For the optimized one-step QW, $\mu_c < 0.57$ eV, and consequently, we must have $\mu_{sc} < 0.57$ eV, if improvement in efficiency is expected.

Unfortunately the proposed QW structures are not deep enough to satisfy thermodynamical demands. If U_b was higher then the μ_{sc}, μ_c could have taken higher values and consequently, the efficiency improvement would be higher. For values of μ_c around 0.8 eV efficiency improvement is around 3%. Also, a higher value of μ_c gives the possibility for higher value of μ_{sc} which is optimal around 7.2 eV.

B. Analysis of the target function

To gain a better understanding of the requirements for the optimal structure, we proceed with the analysis of the target function (Eq. (18)). As presented in Fig. 2, $E_p \approx E_q \approx 0.56$ eV, i.e., $\Delta E \approx 0$. From Eq. (19), it can be concluded that for a small values of ΔE, the integral function increases. However, ΔE determines only the first part of Eq. (19). Therefore, $\Lambda(E)$ and $\Theta(E)$ must also be examined. Those functions are given in Fig. 4 for the optimal quantum well structure from Fig. 2. In the limit $\Gamma_{c1} \rightarrow 0$, the value of $\Theta(E)$ (Eq. (21)) amounts to $\pi\delta(E - E_r)$. Thus, for the small values of Γ_{c1}, $\Theta(E)$ and consequently $D(E)$, have a peak at the energy E_r. This peak can be noticed in Fig. 4, but it is small when compared to the first peak of the sub-integral function $D(E)$. The first peak is usually determined by a peak of $\Lambda(E)$ function, which is always placed very close to the barrier top. This is somewhat expected because the continuous states are slow oscillating at the lower energies part of the continuum spectra. It rises very fast due to phase fitting and then slowly falls down to zero. However, there are cases when the peak at E_r is dominant. Such situation occurs when the pack of $\Lambda(E)$ has smaller values and while the same functions acquire generally higher
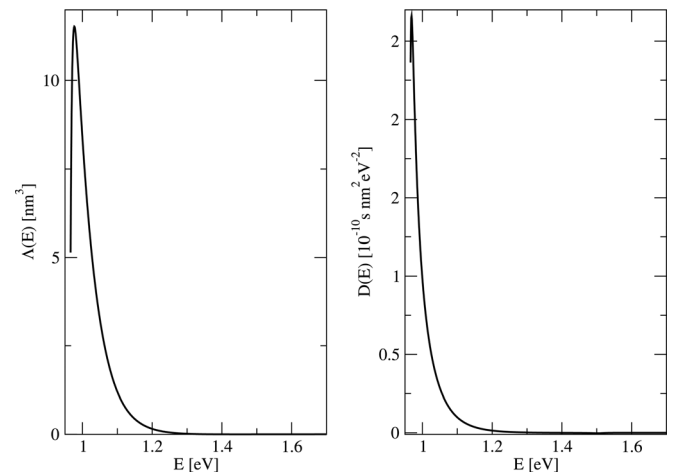

FIG. 4. Left energy function that explicitly involves bound to continuum matrix elements for the optimized step quantum well from Fig. 2. Right: sub-integral function of the energy for the continuum states of the same QW.

values toward the infinity. Which peak is dominant should not be very important for the optimal value of Eq. (18). It turns out that for all the optimized QWs considered here, the first peak is always dominant. It suggests that $D(E)$ is not strongly dependent on the parameter Γ_{c1} which cannot be chosen with high accuracy anyway.

Ideally, for the proposed systems, both peaks should be at the same energy. This could be obtained for deeper QWs. The first peak is always very close to the top of the barrier as indicated in the preceding text. The position of the second peak is determined by the position of the first bound state. In the case of deeper QWs, it is expected that the first bound state is generally around the same position, and therefore E_r is closer to the top of the barrier. As a result, peaks would be multiplied and integral value would be higher.

IV. CONCLUSION

The optical up-converter for enhancing the silicon solar cells efficiency based on the InAs/AlInAs asymmetric step QW structures, taking into account critical layer thickness as constraint, was proposed and optimized. The optimization was done by using the genetic algorithm, which leads to the maximization of target function in the form of second order susceptibility of the QW, for the light frequencies that are suited for the desired photon conversion. The second order susceptibility was derived from the density matrix formalism, while the relevant electron states were calculated using 8-band $\mathbf{k}\cdot\mathbf{p}$ Hamiltonian.

Ideally, QW up-converter should have three bound states where desired nonlinear effect would be more efficient. Unfortunately among zinc-blende III-V materials such QW structure cannot be identified. Therefore, in future work one should seek a material combination that can provide a sufficiently deep well. Possible candidates are wurtzite III-N compounds, which require different modeling. However, the choice of continuum states as the "third state" has proven that the optimization may also be done automatically for nearby continuum states, which would physically improve the nonlinear effect.

[1] M. Green, Prog. Photovoltaics **9**, 123 (2001).
[2] A. Nozik, Physica E. **14**, 115 (2002).
[3] R. R. King, Nat. Photonics **2**, 284 (2008).
[4] A. Luque and A. Martí, Phys. Rev. Lett. **78**, 5014 (1997).
[5] A. Luque, A. Martí, and A. Nozik, MRS Bull. **32**, 236 (2007).
[6] A. Luque and A. Martí, Adv. Mater. **22**, 160 (2010).
[7] S. Tomić, T. S. Jones, and N. M. Harrison, Appl. Phys. Lett. **93**, 263105 (2008).
[8] T. Trupke, M. Green, and P. Wurfel, J. Appl. Phys. **92**, 1668 (2002).
[9] T. Trupke, M. Green, and P. Wurfel, J. Appl. Phys. **92**, 4117 (2002).
[10] B. S. Richards and A. Shalav, IEEE Trans. Electron Devices **54**, 2679 (2007).
[11] Y. Yi, L. Zhu, and Z. Shuai, Macromol. Theory Simul. **17**, 12 (2008).
[12] S. Adachi, in Properties of Semiconductor Alloys-Group-IV, III-V, and II-VI Semiconductors. Wiley Series for Materials for Electronic and Opto-electronic Application (Wiley, New York, 2008), pp. 133–196.
[13] I. Vurgaftman, J. R. Meyer, and L. R. Ram-Mohan, J. Appl. Phys. **89**, 5815 (2001).
[14] I. M. Safonov, I. A. Sukhoivanov, O. V. Shulika, A. A. Dyomin, S. O. Yakushev, M. V. Klymenko, S. I. Petrov, and V. V. Lysak, in Proceedings of ICTON, We.C2.2 IEEE, New York, USA, (2006), pp. 193–198.
[15] S. Kirkpatrick, C. D. Gelatt, and M. P. Vecchi, Science **220**, 671 (1983).
[16] G. Goldoni and F. Rossi, Opt. Lett. **25**, 1025 (2000).
[17] A. Franceschetti and A Zunger, Nature **402**, 60 (1999).
[18] J. Radovanović, V. Milanović, Z. Ikonić, and D. Indjin, J. Phys. D **40**, 5066 (2007).
[19] P. William, T. Saul, V. William, and F. Brian, *Numerical Reciepes in Fortran 90: The Art of Parallel Scientific Computing* (University of Cambridge Press, Cambridge, UK, 1996).
[20] J. Radovanović, V. Milanović, Z. Ikonić, and D. Indjin, Solid State Commun. **110**, 339 (1999).
[21] J. Radovanović, V. Milanović, Z. Ikonić, and D. Indjin, Phys. Rev. B **59**, 5637 (1999).
[22] J. Radovanović, V. Milanović, Z. Ikonić, and D. Indjin, J. Appl. Phys. **91**, 525 (2002).
[23] J. Radovanović, V. Milanović, Z. Ikonić, and D. Indjin, Phys. Rev. B **69**, 115311 (2004).
[24] D. E. Goldberg, *Genetic Algorithms in Search, Optimization and Machine Learning* (Addison-Wesley, Reading, MA, 1989).
[25] S. Tomić, A. G. Sunderland, and I. J. Bush, J. Mater. Chem. **16**, 1963 (2006).
[26] S. Tomić, M. Tadić, V. Milanović, and Z. Ikonić, J. Appl. Phys. **87**, 7965 (2000).
[27] C. Sirtori, F. Capasso, I. Faist and S. Scandolo, Phys. Rev. B **50**, 8663 (1994).
[28] R. V. Boyd, *Nonlinear Optics* (Academic-Elsevier Science, New York, 2003), pp. 129–176.
[29] V. Milanović, Z. Ikonić, and D. Tjapkin, Phys. Low-Dimens. **7**, 65 (1995).
[30] M. F. Pereira, Jr., R. Binder, and S. W. Koch, Appl. Phys. Lett. **64**, 279 (1994).
[31] M. F. Pereira, Jr. and K. Hennerberger, Phys. Stat. Sol. B **202**, 751 (1997).
[32] M. F. Pereira, Jr. and K. Hennerberger, Phys. Stat. Sol. B **206**, 477 (1998).
[33] H. Haug and S. W. Koch, *Quantum Theory of the Optical and Electronic Properties of Semiconductors* (World Scientific Publishing, Singapore, 2004).
[34] M. F. Pereira, Jr., Phys. Rev. B **78**, 245305 (2008).
[35] S. Tomić and E. P. O'Reilly, IEEE Photonic. Technol. Lett. **15**, 6 (2003).
[36] A. Daničić, J. Radovanović, V. Milanović, D. Indjin, and Z. Ikonić, J. Phys. D **43**, 045101 (2010).